TISSUE ENGINEERING
Volume 12, Number 7, 2006

Engineering of Vascularized Transplantable Bone Tissues: Induction of Axial Vascularization in an Osteoconductive Matrix Using an Arteriovenous Loop

ULRICH KNESER, M.D.,[1] ELIAS POLYKANDRIOTIS, M.D.,[1] JAN OHNOLZ,[1] KRISTINA HEIDNER,[1] LUCIA GRABINGER,[1] SIMON EULER,[1] KERSTIN U. AMANN, Ph.D.,[2] ANDREAS HESS, Ph.D.,[3] KAY BRUNE, M.D., Ph.D.,[3] PETER GREIL, Ph.D.,[4] MICHAEL STÜRZL, Ph.D.,[5] and RAYMUND E. HORCH, M.D.[1]

ABSTRACT

Introduction: **Vascularization remains an obstacle to engineering of larger volume bone tissues. Our aim was to induce axial vascularization in a processed bovine cancellous bone (PBCB) matrix using an arteriovenous (AV) loop (artery, vein graft, and vein).** ***Methods:*** **Custom-made PBCB discs (9×5 mm) were implanted into rats. In group A ($n = 19$), the matrices were inserted into microsurgically constructed AV loops between the femoral vessels using a vein graft from the contralateral side. In group B ($n = 19$), there was no vascular carrier. The matrices were encased in isolation chambers. After 2, 4, and 8 weeks, the animals were perfused with India ink via the abdominal aorta. Matrices were explanted and subjected to histological and morphometric analysis. Results were compared with intravital dynamic micro–magnetic resonance imaging and scanning electron microscopy images of vascular corrosion replicas.** ***Results:*** **In group A, significant vascularization of the matrix had occurred by the 8th week. At this time, vascular remodeling with organization into vessels of different sizes was evident. Blood vessels originated from all 3 zones of the AV loop. Group A was significantly superior to group B in terms of vascular density and vascularization kinetics.** ***Discussion:*** **This study demonstrates for the first time successful vascularization of solid porous matrices by means of an AV loop. Injection of osteogenic cells into axially prevascularized matrices may eventually create functional bioartificial bone tissues for reconstruction of large defects.**

INTRODUCTION

BIOARTIFICIAL BONE TISSUES may eventually become alternatives to autologous bone grafts for reconstruction of bone defects.[1,2] A plethora of different cell-based concepts has been reported, whereas differentiation and proliferation of different types of osteogenic cells has been demonstrated *in vitro*.[3–6] Furthermore, a large number of preformed and injectable bone replacement systems have been evaluated under different experimental settings *in vivo*. In these experiments, osteogenic cells induced bone formation in orthotopic and heterotopic locations.[7–10] Porous hydroxyl apatite matrices seeded with bone marrow stromal cells provided bone formation even under clinical conditions.[11]

[1]Department of Plastic and Hand Surgery, University of Erlangen Medical Center, Erlangen, Germany.
[2]Department of Pathology, University of Erlangen Medical Center, Erlangen, Germany.
[3]Department of Pharmacology and Toxicology, University of Erlangen Medical Center, Erlangen, Germany.
[4]Department of Materials Science, Glass and Ceramics, University of Erlangen, Erlangen, Germany.
[5]Department of Molecular and Experimental Surgery, University of Erlangen Medical Center, Erlangen, Germany.

Parts of this work were presented at the 7th International Meeting of the Tissue Engineering Society, October 2004, Lausanne, Switzerland.

Although transplantation of osteogenic bioartificial bone tissues is technically feasible, and some of the currently developed concepts may represent alternatives to autologous bone grafts for certain clinical conditions, the reconstruction of large-volume defects remains challenging. Suboptimal initial vascularization often limits the survival of cells in the center of large cell-containing constructs.[12] Cell-labeling experiments have shown that there is a considerable loss of osteoblasts within the first week after transplantation in porous cancellous bone matrices.[13]

Prefabrication of multi-component flaps is a well-established procedure in plastic surgery.[14,15] Several investigators have described the implantation of vascular carriers into biomaterials for engineering of axially vascularized bone tissues.[16–19] Muscle flaps have also been used for prefabrication of vascularized bone tissues.[20,21] However, in these aforementioned approaches, either matrix-immobilized growth factors were used instead of osteogenic cells, or the vascular carrier was inserted into the matrix at the time of cell transplantation. Insufficient oxygenation and nutrition of cells in the central portions of the matrix immediately after transplantation represent a relevant limitation of many tissue-engineering approaches, particularly when larger volumes of tissues are generated. Therefore the induction of vascularization in biomaterials prior to cell injection (i.e., the prevascularization of scaffolds) may help to increase the initial survival and engraftment of transplanted cells and may consecutively optimize bone formation in bioartificial osteogenic bone tissues.

Erol and Spira described the successful vascularization of a full-thickness skin graft using an arteriovenous (AV) loop in a rat model.[22] Morrison and coworkers, who inserted the loop into isolation chambers, augmented the model.[23,24] They demonstrated the successful induction of vascularization in polymer and gel matrices.[25] Furthermore, the superiority of the AV loop as vascular carrier over the vascular bundle in terms of vascular density and capacity for generation of new tissue was demonstrated.[26] However, the use of an AV loop for the induction of vascularization in porous matrices for engineering of bone tissues has not been described.

Here we present a novel approach for induction of axial vascularization in preformed mechanically stabile matrices suitable for engineering of bone tissues, including a porous processed bovine cancellous bone (PBCB) matrix and an AV loop as vascular carrier. The axial type of vascularization is the opposite of the random pattern type of vascularization that is achieved, for instance, after implantation of biomaterials into subcutaneous pockets. This nomenclature is in accordance with the nomenclature of surgical flaps. Axial vascularization means that 1 vascular axis provides blood supply to a given volume of tissue. Assessment of vascular density and vascularization kinetics demonstrates the successful vascularization of the PBCB matrix. Vascular corrosion casts and micro–magnetic resonance imaging (MRI) are applied for demonstration of functionality and morphologic analysis of the newly generated vascular system. This concept may be applied as a *pre*vascularization strategy to increase survival of osteogenic cells after injection into the matrix.

MATERIALS AND METHODS

Experimental design

The experimental design is outlined in Table 1. Thirty-eight syngenic male Lewis rats were used as recipients. Recipients were divided into 2 groups. In animals from group A ($n = 19$), an AV loop was constructed between the left femoral artery and vein using a contralateral vein graft. A cylindrical PBCB matrix was inserted into the AV loop. The matrix and the loop were placed in an isolation chamber. In group B ($n = 19$), the matrix was placed in the chamber without a vascular carrier. At 2, 4, and 8 weeks after implantation, 5 matrices per group and time were explanted and subjected to histologic and morphometric analysis. Four more matrices per group (1 at 2 weeks, 1 at 4 weeks, and 2 at 8 weeks after implantation) were investigated using intravital high-resolution MRI and consecutive scanning electron microscope of vascular corrosion casts.

Design of matrix and isolation chamber

The design of the isolation chamber and the matrix has been described previously.[27] The cylindrical chamber (inner diameter 10 mm, height 6 mm) with rounded lid was made of heat-resistant medical-grade Teflon in the workshop of the Department of Materials Science, Glass and Ceramics, University of Erlangen. In this study, a commercially available PBCB matrix (Tutobone, Tutogen Medical, Neunkirchen, Germany) was used. A complex processing protocol including fat removal using acetone, ultrasonication, osmotic treatment, oxidation with hydrogen peroxide, and gamma irradiation guarantees removal of donor cells and elimination of cytotoxic agents, antigenicity, and pathogens from the implant. Adhesion, proliferation, and differentiation of osteogenic cells within

Table 1. Experimental Design

	Group A		*Group B*	
	Histology	*MRI/CC-SEM*	*Histology*	*MRI/CC-SEM*
2 weeks	5 (1)	1	5 (2)	1
4 weeks	5	1 (1)	5 (1)	1
8 weeks	5 (1)	2 (1)	5 (1)	2

MRI = high-resolution micro–magnetic resonance imaging.
CC-SEM = corrosion cast + scanning electron microscopy.
Number of animals per group and time are given for each evaluation technique. The number of thrombosed loops in group A and the number of partially infected constructs in group B are given in parentheses.

PBCB matrices and secretion of calcified extracellular matrix have been demonstrated.[6] Because of the biologic origin of the matrix, porosity and pore size are not completely standardized. In our experiments, the porosity of the matrix was approximately 65% to 80% and the pore size 400 to 1000 μm. The dimensions of the custom-made PBCB matrix are 9×5 mm. A 1.5×2.0-mm circular groove accommodates the AV loop. Canals for future injection of gel-immobilized osteoblasts are included in the matrix design (Fig. 1 A, B).

Animal model and surgical procedures

Syngenic male Lewis rats (Charles River Laboratories, Sulzfeld, Germany) served as donors and recipients. German regulations for the care and use of laboratory animals were observed at all times. The animal care committee of the University of Erlangen and the government of Mittelfranken approved all experiments. The animals were housed in the veterinary care facility of the University of Erlangen Medical Center and submitted to a 12-h dark/light cycle with free access to standard chow (Altromin, Hamburg, Germany) and water.

The same micro-surgeon performed all operations under an operative microscope (Karl Zeiss, Jena, Germany). At the commencement of surgery, all rats were given an injection of 0.2 mL of a broad-spectrum depot antibiotic (Tardomycel Comp III, Bayer, Leverkusen, Germany). Operations were performed under Isoflurane (Baxter, Unterschleiβheim, Germany) inhalational anesthesia. The surgical site was shaved, prepped, and draped for sterility. Through a 3- to 4-cm-long skin incision from the groin to the knee, the femoral vessels were fully exposed. Dissection of the vessels extended from the pelvic artery in the groin to the bifurcation of the femoral artery into saphenous and popliteal arteries in the knee. In group A, a 20-mm vein graft was harvested from the right femoral vessels. Interposing the vein graft in original blood-flow direction, an AV loop was created between the proximal stumps of the left femoral artery and vein. The AV loop was placed in the circular groove of the custom-made PBCB matrix. The matrix and the loop were then transferred into the sterile isolation chamber. The lid was closed, and the chamber was fixed in the groin using Vicryl 5–0 (Ethicon, Norderstedt, Germany) sutures. Hemostasis was assured, and the wound was closed using Vicryl 5–0 (Ethicon). In group B, no anastomosis was performed after

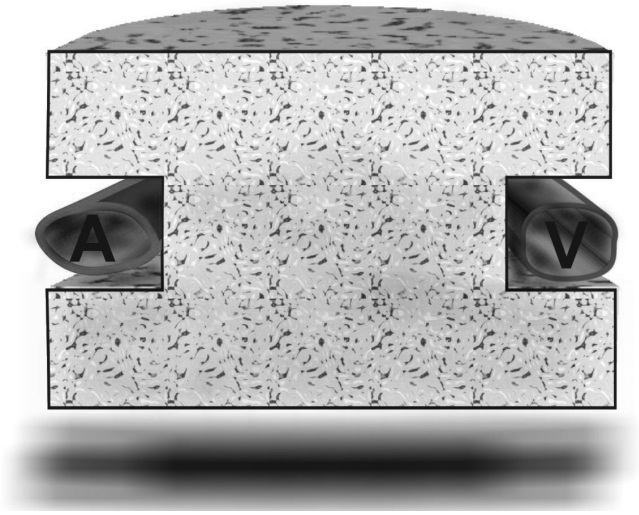

FIG. 1A. Cross section of a matrix from group A. A = artery, V = vein. The arteriovenous loop is placed in a circular groove within the matrix.

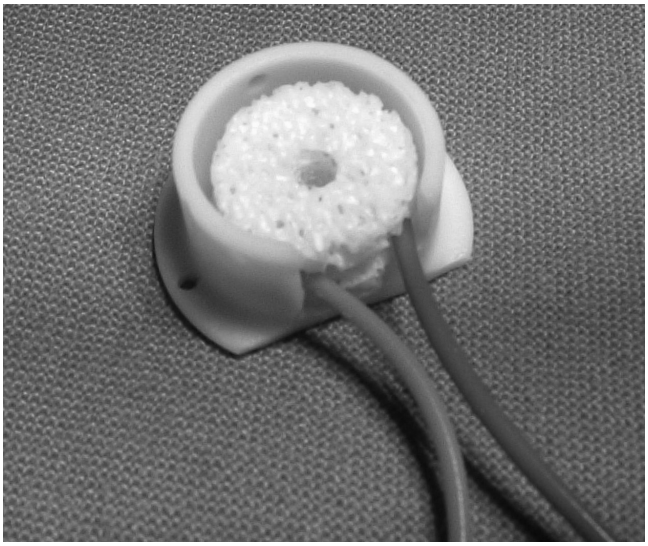

FIG. 1B. Photograph of a matrix encased in the isolation chamber before implantation. The arteriovenous loop is simulated using plastic tubing.

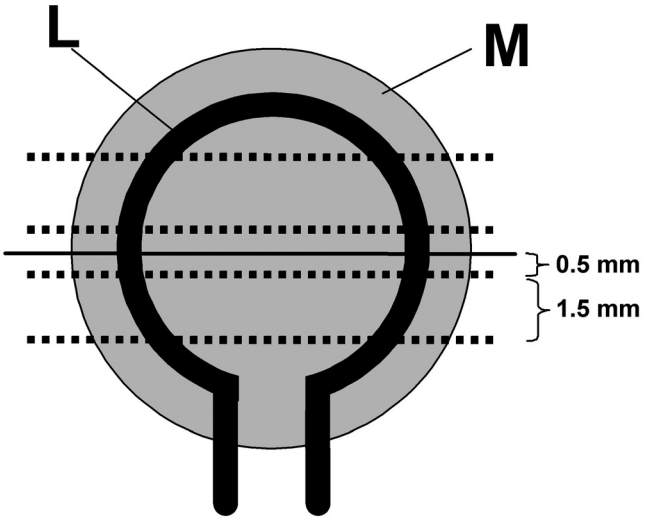

FIG. 1C. Orientation of different planes for histological cross sections. Dashed lines represent planes for histological evaluation. M = matrix, L = AV loop.

dissection of the femoral vessels. The vessels were placed outside of the chamber. The matrix was placed in the isolation chamber as described above.

India ink injection and explantation of the matrices

After induction of anesthesia, the aorta was exposed through a longitudinal laparotomy. The aorta was then cannulated using a 24-gauge catheter and flushed with 100 mL heparin solution in Ringer (100 IE/mL). The inferior vena cava was severed to allow blood and heparin solution to drain. Then, 30 mL of India ink solution (50% v/v India ink, Rohrer, Leipzig, Germany) in 5% gelatin (Roth, Karlsruhe, Germany) and 4% mannitol (Neolab, Heidelberg, Germany) was injected into the abdominal aorta. After setting of the gelatin solution, specimens were macroscopically inspected, explanted, and subjected to histological processing.

Preparation and evaluation of vascular corrosion casts

Vascular corrosion casts were prepared according to a method described by Lametschwandtner *et al.*[28] Briefly, 20 mL of methylmethacrylate monomer was mixed with 1.25 g of catalyst (benzoyl peroxide, Ladd Research, Williston, VT). Six mL of the mixture was combined with 24 mL of Mercox-CL2B (Ladd Research). The resin was injected immediately after mixture. The aorta was exposed and cannulated as described above. The vasculature was rinsed with 100 mL of Ringer-Heparin (100 IE/mL) solution warmed to 37°C until clear backflow from the inferior vena cava was achieved. Twenty mL of the freshly prepared resin was then injected into the aorta under manual pressure control. After perfusion, the catheter was removed and the aorta ligated. The rat cadaver was left in place for 30 min. The vascularized construct still encased in the isolation chamber was then removed and subjected to further processing.

Complete polymerization of the resin was achieved by ''tempering'' in heated distilled water (50°C) for 6 h. The construct was then subjected to 3 cycles of incubation in 7.5% potassium hydroxide (50°C, 12 h) followed by 12 h of rinsing in tap water under gentle continuous flow. The macerated construct was placed in 2% hydrochloric acid at room temperature for another 24 h for decalcification. The cast was placed in 5% formic acid for 15 min at room temperature for final decalcification. Eventually, the cast was rinsed in distilled water and dehydrated in graded ethanol.

The casts were evaluated under a dissecting microscope at a magnification of 25×. In addition, environmental scanning electron microscopy was performed for investigation of the microstructure of the casts. Briefly, specimens were mounted on aluminium stubs using the ''conductive bridge method.'' Measurements were taken under low vacuum conditions, accelerating voltage of 10 kV, in a Philips XL-30 FEG ESEM scanning electron microscope (Philips, Eindhoven, Netherlands).

MRI

MRI was performed on a 4.7 T Bruker Biospec scanner with a free bore of 40 cm, equipped with an actively RF-decoupled coil system. A whole-body birdcage resonator enabled homogenous excitation, and a 3-cm surface coil, located directly above the bone implant to maximize the signal-to-noise ratio, was used as a receiver coil. Angiographic datasets were acquired using a non-triggered 3-dimensional inflow technique (flow-compensated gradient echo sequence, excited slab dimensions were $25.6\times25.6\times25.6$ mm, measured matrix dimensions were $256\times256\times64$, TR = 40 ms, TE = 4.9 ms, 4 averages, flip angle 40°). The volume datasets were evaluated using the MRIan (www.biocom-online.de) and visualized using AMIRA (www.mc.com/tgs). Because of the MR inflow technique, high signal intensities (bright voxels) correspond to blood flow from vessels, as well as perfused regions in general. These high-intensity regions can be visualized using so-called maximum intensity projections and isosurface renderings. A newly developed semi-automatic vessel segmentation and reconstruction algorithm (Gaudnek *et al.,* 2005, IEEE ICIP, in press) dedicated to MR angiography allowed the extraction of large parts of the blood vessels supplying the bone implant. For MRI investigation, the animals were anesthetized using Isofluran. The measuring period was 1 h 30 min. The animals recovered quickly and continued the full experimental period.

Histological and statistical analysis

Specimens were explanted *in toto*, fixed in formalin, dehydrated in graded ethanol, and embedded in paraffin. Five-μm cross sections were obtained from 4 standardized planes (2 central, 1 proximal, and 1 distal) using a Leica microtome (Leica Microsystems, Bensheim, Germany) (Fig. 1C). All planes were oriented perpendicular to the longitudinal axis of the AV loop. Sections were stained using hematoxylin eosin according to standard protocols. Microphotographs were taken using an Axioplan microscope and Axiocam digital camera (Carl Zeiss, Oberkochen, Germany); no digital processing of the original pictures was performed at any time.

Blood vessel density was quantified in 4 planes per implant. India ink–filled (positive) vessels were counted in 10 high-power (×200) fields that a blinded observer randomly selected according to a defined grid scheme in defined sectors. The cross section was divided into 3 rows. The central row contained 4 sectors, 2 each close to the artery and vein. The upper and lower rows comprised 3 sectors. The mean value of blood vessel counts per field was calculated for any group and any time. Results are given as mean ± standard deviation. Statistical analysis was performed using GraphPad Prism software. Two-tailed unpaired Student's *t*-test was applied for statistical analysis. The critical level of statistical significance chosen was $p < 0.05$.

RESULTS

Feasibility of the implantation procedures and microsurgical vascular anastomosis

All of the 38 recipients tolerated the surgical procedures well. There were neither anesthesia-related deaths nor major surgical complications. In 7 of the animals, a hematoma could be evacuated by puncture during the initial postoperative period. Upon explantation, the isolation chambers appeared wrapped in a thin capsule of fibrous tissue. Four implants from group B (2 at 2 weeks, 1 at 4 weeks, and 1 at 8 weeks after implantation) displayed macroscopic signs of infection at the distal pole of the construct opposite the opening of the isolation chamber.

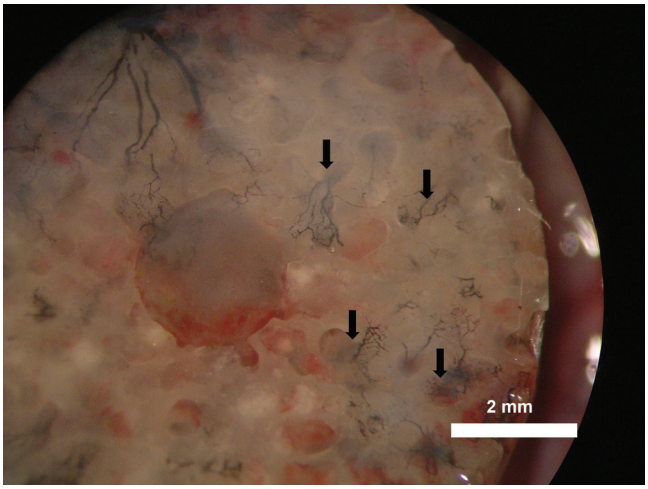

FIG. 2A. Matrix from group A (arteriovenous loop) 8 weeks after implantation. India ink injection demonstrates infiltration of pores of the matrix with a network of small blood vessels originating from the axial vascular carrier in the depth (arrows).

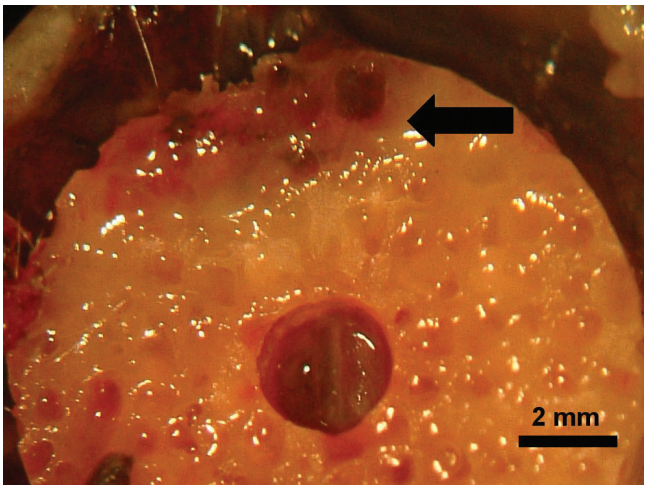

FIG. 2B. Matrix from group B (control) 8 weeks after implantation. Only small vessels close to the opening of the chamber can be seen using India ink injection (arrow). (Color images available online at www.liebertpub.com/ten.)

Blood vessels in the implants are functionally intact

In group A, patency of 15 of 19 AV loops was demonstrated using India ink injection or injection of methylmethacrylate polymer. In these specimens, blood vessels invaded the pores of the entire matrix (Fig. 2A). Macroscopically, the degree of vascularization increased over the course of the experiment. In group B, vascularization was evident only in the region close to the opening of the chamber (Fig. 2B). In 4 constructs from group A, the AV loop was

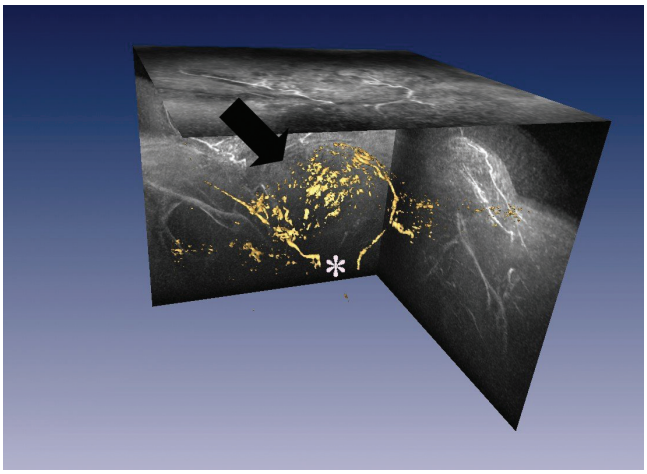

FIG. 3A. Micro–magnetic resonance imaging of a matrix from group A at 8 weeks after implantation. Shown are the 3 orthogonal maximum intensity projections through the data volume acquired with a 3D inflow angiographic sequence. Voxel resolution: $100\times 100\pm 400\,\mu m$. Additional isosurface rendering shows regions of high voxel intensities (i.e., regions with high blood flow). In addition to the arteriovenous loop (asterisk), the arrow indicates the perfused tissue volume within the isolation chamber.

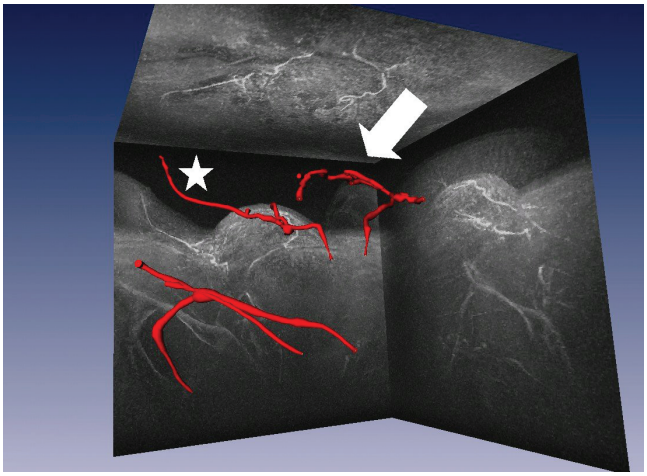

FIG. 3B. Micro–magnetic resonance imaging of a matrix from group A at 8 weeks after implantation. By using a semiautomatic vessel segmentation algorithm, the larger vessels were segmented, reconstructed, and visualized as geometric primitives. Arrow indicates the arteriovenous loop around the matrix. Star indicates the epigastric artery. (Color images available online at www.liebertpub.com/ten.)

thrombosed. However, these matrices also displayed macroscopic signs of vascularization.

Perfusion of the matrices from group A could be verified using intravital MRI examination. The volume of perfused tissue within the chamber was detected using the high signal intensity (Fig. 3A). Only in group A could MRI demonstrate a vascular axis. The vessels supplying the construct could easily be segmented (Fig. 3B). The existence of a vessel loop in the MR inflow angiography clearly demonstrates the blood flow within and functional integrity of this vessel. In 2 matrices (1 at 4 and 1 at 8 weeks after implantation), no vascular axis was visible in the MRI scan. Corrosion cast evaluation demonstrated occlusion of the AV loop in these animals. In group B, no significant perfusion of the matrix and no defined vascular axis were detectable over the observation period using MRI.

An organized capillary network is formed in the axially vascularized matrices

Vascular corrosion casts were prepared for assessment of the morphology of the vascular system within the matrix. The vascularization seemed to be the lowest in the graft portion of the loop (Fig. 4A). However, capillaries sprouted from all parts of the loop, including the graft segment. At higher magnification, luminal sprouting from all areas of the loop was evident. Furthermore, there was vascular expansion with vessels of different calibers from the vasa vasorum of the vascular axis (Fig. 4B). In the 4- and 8-week specimens, especially at the proximal segments (near the arterial part), the neo-vascular beds were oriented parallel to the vascular axis, as an adaptation to higher pulsatile pressure

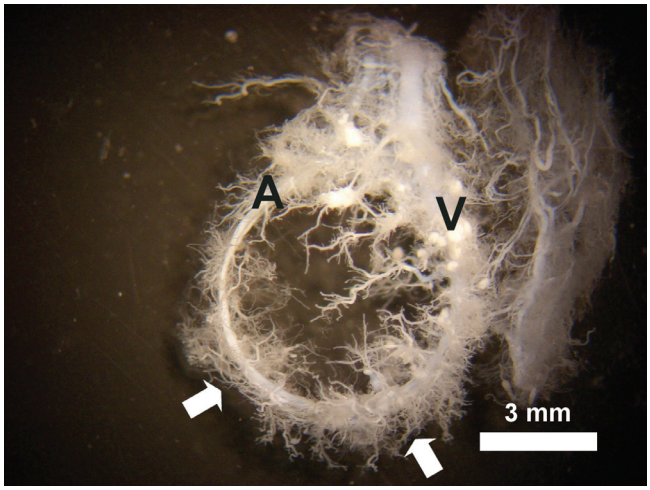

FIG. 4A. Vascular corrosion cast of a construct from group A (8 weeks after implantation). Blood vessels of different sizes originate from the circular arteriovenous loop. A higher vascular density is observed in the venous region of the loop than in the vein graft or the arterial region. Arrows indicate the site of the anastomosis between the vein graft and the vascular pedicle. A = artery, V = vein.

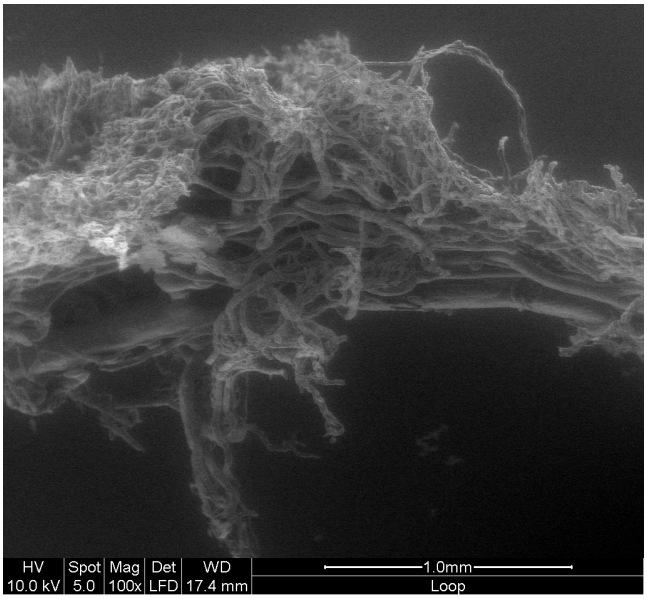

FIG. 4B. Luminal sprouts originate from the axial vessels of the arteriovenous loop and from the vasa vasorum. Scanning electron microscopy ×100.

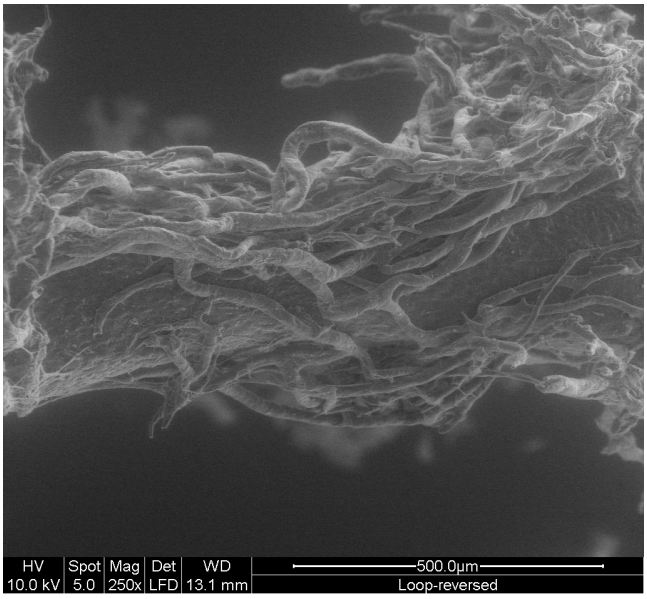

FIG. 4C. The neo-vascular beds are oriented parallel to the vascular axis as an adaptation to a higher pulsatile pressure. Scanning electron microscopy ×250. (Color images available online at www.liebertpub.com/ten.)

(Fig. 4C). In the 8-week specimens, the vascular network showed an increased variability in caliber, possibly due to remodeling of the vascular structures.

Vascular density in the matrices increases after insertion of a vascular carrier

Histologic evaluation of implanted matrices demonstrates an increase of vascularization over time in the AV loop

group A. By 2 weeks, the pores of the matrix in group A were filled with a fibrin meshwork. The vascular axis gave rise to many capillaries and some larger blood vessels. The formation of vascularized connective tissue was limited to the circular groove of the matrix. After 4 weeks, the matrices displayed a significant degree of vascularization. Originating from the vascular axis, a dense network of ink-filled blood vessels invaded the pores of the matrix. The amount of connective tissue and the vascular density within the matrix pores decreased as it progressed from the vessels of the vascular axis toward the peripheral regions. The newly formed tissue within the pores of the matrix was composed of inflammatory cells, fibroblasts, blood vessels, and vascular sprouts. Between 4 and 8 weeks, the vascularized tissue continued to grow centripetally toward the periphery of the vascular axis (Fig. 5A). The degree of vascularization increased considerably during this time. The maturation of the newly formed connective tissue was obvious between 4 and 8 weeks. Patency of the vessels and continuity with the AV loop were visualized using India ink perfusion at all times. Direct luminal sprouting from the vascular axis was evident (Fig. 5B). A high degree of vascularization could be demonstrated even in central regions of the matrix at 8 weeks after implantation (Fig. 5C). The 4 constructs with thrombosed AV loop also displayed a vascular network within the pores of the matrix. However, the density of the blood vessels was considerably lower in these constructs than in the ones with patent AV loops.

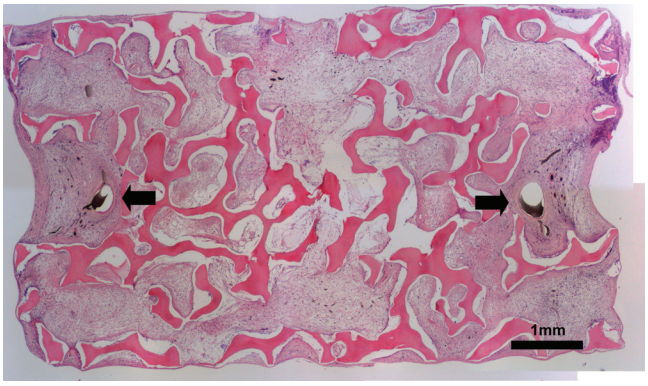

FIG. 5A. Cross section of a matrix from group A (arteriovenous (AV) loop) at 8 weeks. India ink injection demonstrates a high degree of vascularization within the whole matrix. The vascular axis (AV loop, arrows) is placed in the groove of the matrix and embedded in highly vascularized connective tissue (hematoxylin eosin staining).

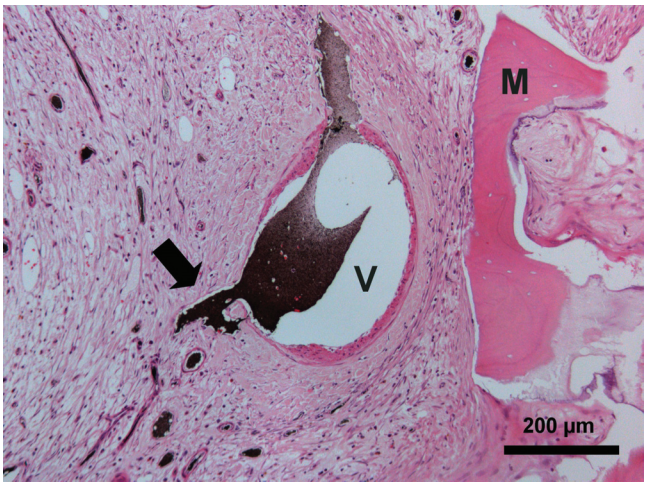

FIG. 5B. Luminal sprouting from the venous (V) part of the loop is clearly visible (arrow). M = matrix. (Group A, India ink injection + hematoxylin eosin staining, 8 weeks.)

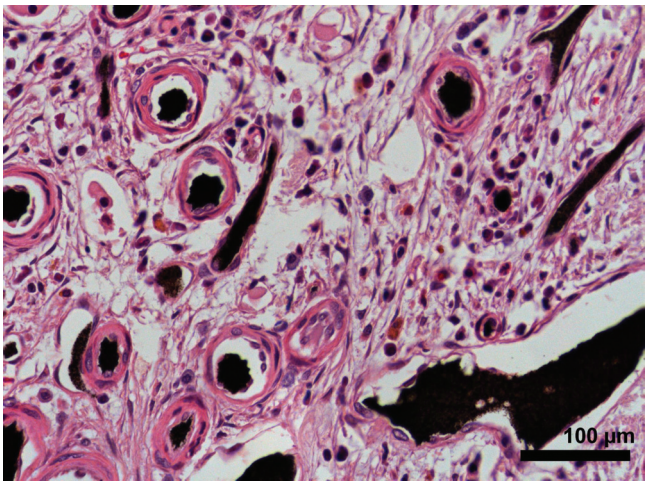

FIG. 5C. Even the central pores of the matrix are filled with cell-rich, highly vascularized connective tissue. (Group A, India ink injection + hematoxylin eosin staining, 8 weeks.)

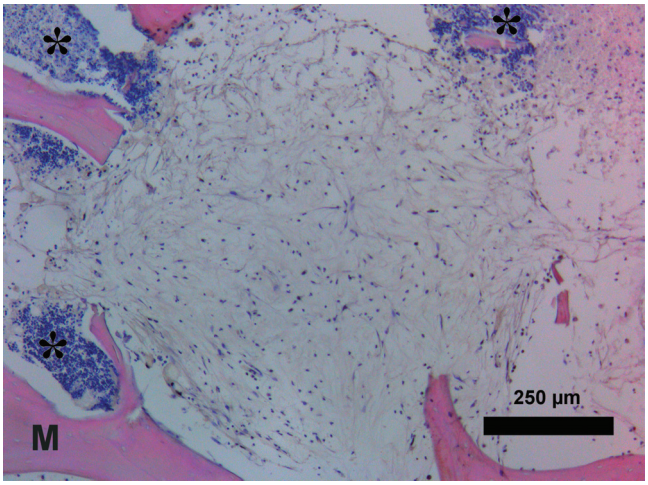

FIG. 5D. In control group B, only the pores of the matrix (M) in proximity to the opening of the chamber are filled with loose connective tissue. This tissue does not contain significant numbers of black-stained blood vessels. Agglomerations of granulocytes (asterisks) are evident in contact with the matrix. (India ink injection + hematoxylin eosin staining, 8 weeks.) (Color images available online at www.liebertpub.com/ten.)

In group B, there was virtually no vascularization at 2 weeks after implantation. Tissue formation and vascularization progressed from the opening of the isolation chamber toward the periphery between 4 and 8 weeks. However, the amount of tissue formation and vascularization was significantly lower in group B than in group A (Fig. 5D). At 4 and 8 weeks, a proportion of the implants displayed signs of infection such as abscess formation. However, infections were limited to the distal proportion of the matrix opposite the opening of the isolation chamber. There was no foreign body reaction visible at any time.

Quantitative analysis of blood vessel density demonstrated a significant, continuous increase in the amount of vascularization between week 2 and week 8 after implantation in axially vascularized implants from group A (2 weeks 8.88 ± 19.86; 4 weeks 56.02 ± 25.06; 8 weeks 107.0 ± 57.2; $p < 0.05$) (Fig. 6). In group B (control), no vascularization could be observed at 2 weeks after implantation. At 4 and 8 weeks after implantation, there was only minimal vascularization in the proximal parts of the implants (close to the opening of the chamber) detectable (2 weeks 0 ± 0; 4 weeks 13.88 ± 18.88; 8 weeks 13.48 ± 11.82). At 4 and 8 weeks, the difference between groups A and B was statistically significant ($p < 0.05$).

DISCUSSION

Using this isolation chamber model, we demonstrated for the first time successful axial vascularization of biogenic, mechanically stabile matrices for bone tissue engineering by insertion of an AV loop. In this study we adopted the concept of Morrison and coworkers[23,24,26,29] for the generation of vascularized bone tissue.

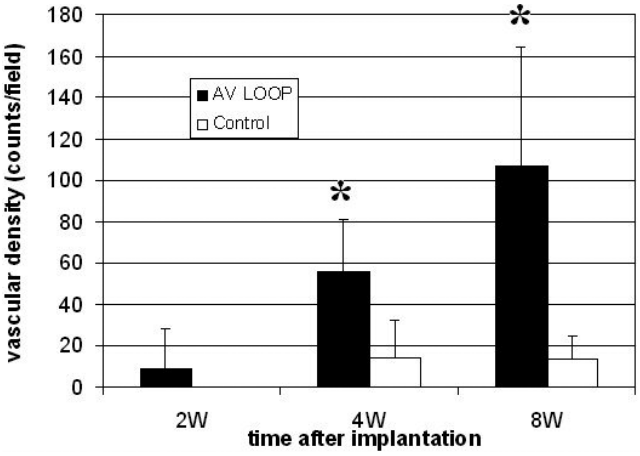

FIG. 6. Quantification of vascular density. Vascular density is given in counts per field as mean ± standard deviation. Each bar represents 5 specimens. Forty fields were assessed per specimen in 4 defined planes. Asterisk indicates statistical difference between group A (arteriovenous loop) and group B (control).

Historically, the principles of flap prefabrication[14] were applied to the generation of axially vascularized bone tissues. The latissimus dorsi muscle has been described as carrier for prefabricated bone flaps.[17] Recently, this concept has been successfully applied in combination with bone morphogenetic protein (BMP)-2 in a clinical setting for the reconstruction of a mandibular defect after cancer resection and irradiation.[21] Although this technique works well in practice, it has the disadvantage of potential donor site morbidity of the latissimus dorsi flap harvest. The use of isolated vascular bundles appears more suitable than muscle flaps as a carrier for bone tissues because the morbidity of an isolated blood vessel harvest is presumably lower than the one of a muscle flap harvest. Several vessels have been used for prefabrication of axially vascularized bone flaps in different animal models.[16,18,19,30] Akita *et al.* implanted the femoral vascular pedicle into BMP-2–loaded porous hydroxyapatite ceramics and observed better vascularization and bone formation than with subcutaneously implanted constructs in a rat model.[31] The saphenous bundle was also used in a rat model to enhance bone formation in subcutaneously implanted cancellous bone grafts and bone marrow after bed isolation with biodegradable membranes.[19]

Erol and Spira described the prefabrication of axially vascularized skin flaps based on AV loops as early as 1979.[22] In the late 1990s, Morrison and coworkers[26] evaluated the capacity of femoral vascular bundles versus that of the AV loop with regard to tissue formation and vascularization. In this study, the AV loop provided a higher degree of vascularization within the matrix. From the plastic surgeon's point of view, the AV loop is associated with minimal donor site morbidity. It may be created at any surgical site and has no limitations in terms of pedicle length because the venous graft easily bridges the gap between artery and vein at the vascular pedicle. Therefore the creation of multi-compound flaps including bone and skin tissue seems technically feasible.

The evaluation of vascularization is a complex problem. Histological techniques have been applied for decades and provide, in combination with ink injection and adequate morphometric analysis, insight into vascularization processes within tissues. The preparation of vascular replicas (corrosion casts) allows the assessment of vascular tree morphology and spatial distribution of vessels within 3-dimensional matrices and represents a valuable tool for the study of tissue neogenesis based on vascular carriers.[32] In the presented experimental setting, the matrices from group A were almost completely infiltrated with vascularized connective tissue at 8 weeks after implantation of the AV loop as demonstrated by histology (Fig. 5A). The technique of cast preparation caused the apparently incomplete pattern of vascularization with a central gap (Fig. 4A) in vascular corrosion casts of matrices from group A. Because of the viscosity of the polymer, capillaries and very small vessels that are mainly located at a distance from the vascular axis could not be visualized.

Histology and corrosion casting represent static techniques for assessment of vascularization of porous matrices. Therefore, we additionally performed intravital high-resolution MRI for dynamic evaluation of circulation within the constructs. This technique has been described for evaluation of ectopic bone formation in rats after subcutaneous implantation of demineralized bone matrix.[33] In contrast to Hartman *et al.,* we were able to visualize single blood vessels within the matrix after processing of the high-resolution images using a newly developed vessel segmentation algorithm (Gaudnek *et al.,* 2005, IEEE ICIP, in press). In this study, using the high-resolution micro-MRI, it was possible to non-invasively detect occlusion of the vascular axis within the isolation chamber. In the future, even long-term monitoring of tissue generation within isolation chambers seems technically feasible because each individual animal can be investigated at several time points using the non-invasive micro-MRI technique. The different dynamic and static evaluation tools applied in this study allowed for a detailed assessment of the vascularization patterns within the PBCB matrices.

In the present study, there were considerable microscopic and macroscopic differences between axially vascularized and non-vascularized (control) constructs. In the experimental group A, we observed the development of a constantly growing and maturating vascular system within the matrix. Interestingly, each part of the AV loop contributed to this vascularization process. Evaluation of vascular corrosion casts clearly demonstrated that not only the venous and arterial portion but also the graft portion of the loop gave rise to new blood vessels. This is an interesting finding with regard to flap prefabrication strategies in clinical settings. Although we were able to demonstrate successful penetration of the porous construct with new blood vessels, the relevance of this finding with regard to future applications in reconstructive surgery is unclear. The observed vascular ingrowth might protect the biomaterial from infections at the recipient site. Furthermore, the newly formed vascular system may enhance bone formation after injection of osteogenic cells or application of osteoinductive growth factors.

However, clinical applications of axially vascularized processed cancellous bone matrices require quick, efficient, and reliable vascularization of large scaffold volumes. The capacity of AV loops as vascular carrier for vascularization of larger matrix volumes is unclear. Extrapolation from small animal models harbors the risk of unpredictable overestimation of the vascularization properties because neither the matrix geometry nor the tissue-matrix-loop interactions are comparable. Therefore, larger-animal experiments with regard to upscaling of the presented model are the subject of ongoing research in our laboratory.

It is possible that growth factors such as vascular endothelial growth factor or basic fibroblast growth factor may further enhance the vascularization of porous matrices. In contrast to group A (AV loop), matrices from the control group B did not contain any axially oriented blood vessels over the whole observation period. Furthermore, we did not observe morphological signs of maturation of the few blood vessels within the construct. The quantitative analysis of vascular density reflects the insufficient vascularization of these matrices, especially of the distal parts without contact with the opening of the chamber. In this analysis, there was no increase in vascularization between 4 and 8 weeks after implantation in the control group, in contrast to the AV-loop group A. In our opinion, the insufficient perfusion of the tissue also caused the macroscopically visible infection in 4 of 19 matrices from the control group B at the distal portion of the implants. Others have previously described this phenomenon in a comparable experimental setting.[32]

Prevascularization strategies have gained rising interest in the field of tissue engineering because a well-vascularized environment represents a prerequisite for successful cell engraftment and consecutive organ-specific function of the transplanted cells. Although prevascularization techniques have been described for engineering of organs based on cells with high metabolic activity, such as hepatocytes, this concept has not been sufficiently addressed with regard to application in engineering of bone tissues. The axial type of vascularization, which is also referred to as an intrinsic type of vascularization, allows the vascularization and transfer of biomaterials independent of local conditions at the recipient site. To our knowledge, no studies focusing on transplantation of osteogenic cells into solid mechanically stable porous matrices after induction of axial vascularization have been published. In the future, the presented approach, which combines tissue-engineering strategies with plastic surgical techniques, will allow the injection of organ-specific cells into prevascularized matrices to create custom-made bioartificial axially vascularized flaps. The application of growth factors such as BMPs may further enhance bone formation in the newly formed vascularized tissues. Eventually, these neo-tissues may be used for complex reconstructions with minimal donor site morbidity.

CONCLUSION

This study demonstrates for the first time the induction of axial vascularization in a biomaterial suitable for engineering of bone tissues using an AV loop as vascular carrier. The next step will be the injection of osteogenic cells into the prevascularized matrices. Eventually this concept may facilitate the generation of large volumes of vascularized bone tissues suitable for reconstruction of bone defects even under problematic clinical circumstances.

ACKNOWLEDGMENTS

This work contains parts of E. Polykandriotis' doctoral thesis. A. Lametschwandtner's instruction in the corrosion

cast technique is highly appreciated. The authors thank T. Fey and E. Springer for the investigations using the scanning electron microscope. This study was supported by research grants from the University of Erlangen (ELAN Program and the IZKF) and from Tutogen Medical Inc.

REFERENCES

1. Cancedda, R., Dozin, B., Giannoni, P., and Quarto, R. Tissue engineering and cell therapy of cartilage and bone. Matrix Biol **22,** 81, 2003.
2. Kneser, U., Schaefer, D. J., Munder, B., Klemt, C., Andree, C., and Stark, G. B. Tissue engineering of bone. Min Invas Sur Allied Technol **11,** 107, 2002.
3. Schantz, J. T., Teoh, S. H., Lim, T. C., Endres, M., Lam, C. X., and Hutmacher, D. W. Repair of calvarial defects with customized tissue-engineered bone grafts. I. Evaluation of osteogenesis in a three-dimensional culture system. Tissue Eng **9 Suppl 1**, S113, 2003.
4. Arnold, U., Lindenhayn, K., and Perka, C. In vitro cultivation of human periosteum derived cells in bioresorbable polymer-TCP-composites. Biomaterials **23,** 2303, 2002.
5. Effah Kaufmann, E. A., Ducheyne, P., and Shapiro, I. M. Evaluation of osteoblast response to porous bioactive glass (45S5) substrates by RT-PCR analysis. Tissue Eng **6,** 19, 2000.
6. Stangenberg, L., Schaefer, D. J., Buettner, O., Ohnolz, J., Moebest, D., Horch, R. E., Stark, G. B., and Kneser, U. Differentiation of osteoblasts in three-dimensional culture in porous cancellous bone matrix: quantitative analysis of gene expression based on real-time reverse transcription polymerase chain reaction. Tissue Eng **11,** 855, 2005.
7. Temenoff, J. S., and Mikos, A. G. Injectable biodegradable materials for orthopedic tissue engineering. Biomaterials **21 AB,** 2405, 2000.
8. Kneser, U., Voogd, A., Ohnolz, J., Zhang, Y. H., Stark, G. B., and Schaefer, D. J. Fibrin gel-immobilized primary osteoblasts in calcium phosphate bone cement: in vivo evaluation with regard to application as injectable biological bone substitute. Cells Tissues Organs **179,** 158, 2005.
9. Schantz, J. T., Hutmacher, D. W., Lam, C. X., Brinkmann, M., Wong, K. M., Lim, T. C., Chou, N., Guldberg, R. E., and Teoh, S. H. Repair of calvarial defects with customised tissue-engineered bone grafts II. Evaluation of cellular efficiency and efficacy in vivo. Tissue Eng **9 Suppl 1,** S127, 2003.
10. Yamada, Y., Boo, J. S., Ozawa, R., Nagasaka, T., Okazaki, Y., Hata, K., and Ueda, M. Bone regeneration following injection of mesenchymal stem cells and fibrin glue with a biodegradable scaffold. J Craniomaxillofac Surg **31,** 27, 2003.
11. Quarto, R., Mastrogiacomo, M., Cancedda, R., Kutepov, S. M., Mukhachev, V., Lavroukov, A., Kon, E., and Marcacci, M. Repair of large bone defects with the use of autologous bone marrow stromal cells. N Engl J Med **344,** 385, 2001.
12. Kneser, U., Kaufmann, P. M., Fiegel, H. C., Pollok, J. M., Kluth, D., Herbst, H., and Rogiers, X. Long-term differentiated function of heterotopically transplanted hepatocytes on three-dimensional polymer matrices. J Biomed Mater Res **47,** 494, 1999.
13. Kneser, U., Stangenberg, L., Ohnolz, J., Buettner, O., Stern-Strater, J., Moebest, D., Horch, R. E., Stark, G. B., and Schaefer, D. J. Reconstruction of critical size calvarial defects using processed bovine cancellous bone matrix and autologous osteoblasts. J Cell Mol Med, accepted, 2006.
14. Khouri, R. K., Upton, J., and Shaw, W. W. Principles of flap prefabrication. Clin Plast Surg **19,** 763, 1992.
15. Schipper, J., Ridder, G. J., Maier, W., and Horch, R. E. [The preconditioning and prelamination of pedicled and free microvascular anastomised flaps with the technique of vacuum assisted closure]. Laryngorhinootologie **82,** 421, 2003.
16. Lee, J. H., Cornelius, C. P., and Schwenzer, N. Neo-osseous flaps using demineralized allogeneic bone in a rat model. Ann Plast Surg **44,** 195, 2000.
17. Casabona, F., Martin, I., Muraglia, A., Berrino, P., Santi, P., Cancedda, R., and Quarto, R. Prefabricated engineered bone flaps: an experimental model of tissue reconstruction in plastic surgery. Plast Reconstr Surg **101,** 577, 1998.
18. Gill, D. R., Ireland, D. C., Hurley, J. V., and Morrison, W. A. The prefabrication of a bone graft in a rat model. J Hand Surg [Am] **23,** 312, 1998.
19. Hokugo, A., Kubo, Y., Takahashi, Y., Fukuda, A., Horiuchi, K., Mushimoto, K., Morita, S., and Tabata, Y. Prefabrication of vascularized bone graft using guided bone regeneration. Tissue Eng **10,** 978, 2004.
20. Terheyden, H., Menzel, C., Wang, H., Springer, I. N., Rueger, D. R., and Acil, Y. Prefabrication of vascularized bone grafts using recombinant human osteogenic protein-1—part 3: dosage of rhOP-1, the use of external and internal scaffolds. Int J Oral Maxillofac Surg **33,** 164, 2004.
21. Warnke, P. H., Springer, I. N., Wiltfang, J., Acil, Y., Eufinger, H., Wehmoller, M., Russo, P. A., Bolte, H., Sherry, E., Behrens, E., and Terheyden, H. Growth and transplantation of a custom vascularised bone graft in a man. Lancet **364,** 766, 2004.
22. Erol, O. O., and Spira, M. New capillary bed formation with a surgically constructed arteriovenous fistula. Surg Forum **30,** 530, 1979.
23. Mian, R., Morrison, W. A., Hurley, J. V., Penington, A. J., Romeo, R., Tanaka, Y., and Knight, K. R. Formation of new tissue from an arteriovenous loop in the absence of added extracellular matrix. Tissue Eng **6,** 595, 2000.
24. Hofer, S. O., Knight, K. M., Cooper-White, J. J., O'Connor, A. J., Perera, J. M., Romeo-Meeuw, R., Penington, A. J., Knight, K. R., Morrison, W. A., and Messina, A. Increasing the volume of vascularized tissue formation in engineered constructs: an experimental study in rats. Plast Reconstr Surg **111,** 1186, discussion 1193, 2003.
25. Cassell, O. C., Morrison, W. A., Messina, A., Penington, A. J., Thompson, E. W., Stevens, G. W., Perera, J. M., Kleinman, H. K., Hurley, J. V., Romeo, R., and Knight, K. R. The influence of extracellular matrix on the generation of vascularized, engineered, transplantable tissue. Ann N Y Acad Sci **944,** 429, 2001.
26. Tanaka, Y., Sung, K. C., Tsutsumi, A., Ohba, S., Ueda, K., and Morrison, W. A. Tissue engineering skin flaps: which vascular carrier, arteriovenous shunt loop or arteriovenous bundle, has more potential for angiogenesis and tissue generation? Plast Reconstr Surg **112,** 1636, 2003.
27. Kneser, U., Polykandriotis, E., Ohnolz, J., Heidner, K., Bach, A. D., Kopp, J., and Horch, R. E. Vascularized bone replacement for the treatment of chronic bone defects-initial

results of microsurgical hard tissue vascularization. Zeitschr Wundheilung **4,** 62, 2004.
28. Lametschwandtner, A., Lametschwandtner, U., and Weiger, T. Scanning electron microscopy of vascular corrosion casts—technique and applications: updated review. Scanning Microsc **4,** 889, discussion 941, 1990.
29. Tanaka, Y., Tsutsumi, A., Crowe, D. M., Tajima, S., and Morrison, W. A. Generation of an autologous tissue (matrix) flap by combining an arteriovenous shunt loop with artificial skin in rats: preliminary report. Br J Plast Surg **53,** 51, 2000.
30. Mankani, M. H., Krebsbach, P. H., Satomura, K., Kuznetsov, S. A., Hoyt, R., and Robey, P. G. Pedicled bone flap formation using transplanted bone marrow stromal cells. Arch Surg **136,** 263, 2001.
31. Akita, S., Tamai, N., Myoui, A., Nishikawa, M., Kaito, T., Takaoka, K., and Yoshikawa, H. Capillary vessel network integration by inserting a vascular pedicle enhances bone formation in tissue-engineered bone using interconnected porous hydroxyapatite ceramics. Tissue Eng **10,** 789, 2004.
32. Bernard, S. L., and Picha, G. J. The use of coralline hydroxyapatite in a ''biocomposite'' free flap. Plast Reconstr Surg **87,** 96, discussion 106, 1991.
33. Hartman, E. H., Pikkemaat, J. A., Vehof, J. W., Heerschap, A., Jansen, J. A., and Spauwen, P. H. In vivo magnetic resonance imaging explorative study of ectopic bone formation in the rat. Tissue Eng **8,** 1029, 2002.

Address reprint requests to:
Ulrich Kneser, M.D.
Department of Plastic and Hand Surgery
University of Erlangen Medical Center
Krankenhausstrasse 12
91054 Erlangen
Germany

E-mail: ulrich.kneser@chir.imed.uni-erlangen.de